Reinig, F. and Wacker, L. and Joris, O. and Oppenheimer, C. and Guidobaldi, G. and Nievergelt, D. and Adolphi, F. and Cherubini, P. and Engels, Stefan and Esper, J. and Land, A. and Lane, C. and Pfanz, H. and Remmele, S. and Sigl, M. and Sookdeo, A. and Buntgen, U. (2021) Precise date for the Laacher See eruption synchronizes the Younger Dryas. Nature 595 , pp. 66-69. ISSN 0028-0836.

Precise date for the Laacher See eruption synchronizes the Younger Dryas

Frederick Reinig[1,*], Lukas Wacker[2], Olaf Jöris[3,4,5], Clive Oppenheimer[6], Giulia Guidobaldi[7], Daniel Nievergelt[7], Florian Adolphi[8,9], Paolo Cherubini[7,10], Stefan Engels[11], Jan Esper[1], Alexander Land[12,13], Christine Lane[6], Hardy Pfanz[14], Sabine Remmele[12], Michael Sigl[15], Adam Sookdeo[2], Ulf Büntgen[6,7,16,17]

[1]Department of Geography, Johannes Gutenberg University, Mainz, Germany, [2]ETH Zurich, Laboratory of Ion Beam Physics, Zurich, Switzerland, [3]Römisch-Germanisches Zentralmuseum - MONREPOS Archaeological Research Centre and Museum for Human Behavioural Evolution, Neuwied, Germany, [4]Institute of Ancient Studies, Department of Prehistoric and Protohistoric Archaeology, Johannes Gutenberg University, Mainz, Germany, [5]MOE Key Laboratory of Western China's Environmental Systems Research School of Arid Environment and Climate Change, Lanzhou, China, [6]Department of Geography, University of Cambridge, Cambridge, UK, [7]Swiss Federal Research Institute WSL, Birmensdorf, Switzerland, [8]Alfred Wegener Institute, Helmholtz Center for Polar and Marine Research, Bremerhaven, Germany, [9]Department of Geosciences, University of Bremen, Bremen, Germany, [10]Department of Forest and Conservation Sciences, University of British Columbia, Vancouver BC, Canada, [11]Department of Geography, Birkbeck University of London, London, UK, [12]University of Hohenheim, Institute of Biology (190a), Stuttgart, Germany, [13]University of Applied Forest Sciences, Rottenburg am Neckar, Germany, [14]Institute of Applied Botanics and Volcanic Biology, Universität Duisburg-Essen, Essen, Germany, [15]Climate and Environmental Physics, Physics Institute, and Oeschger Centre for Climate Change Research, University of Bern, Bern, Switzerland, [16]Global Change Research Institute of the Czech Academy of Sciences (CzechGlobe), Brno, Czech Republic, [17]Department of Geography, Faculty of Science, Masaryk University, Brno, Czech Republic.

*e-mail: reinig@geo.uni-mainz.de

The Laacher See Eruption (LSE) ranks among Europe's largest Upper Pleistocene volcanic events[1,2]. Although its tephra deposits represent an important isochron for the synchronisation of proxy archives at the Late Glacial to early Holocene transition[3], uncertainty in the eruption age has prevailed[4]. Here, we present dendrochronological and radiocarbon measurements of subfossil trees buried by pyroclastic deposits that firmly date the LSE to 13,006 ± 9 cal BP, more than a century earlier than hitherto accepted. The revised age of the LSE, now the oldest volcanic eruption worldwide dated with such precision, necessarily shifts the chronology of European varved lakes[5,6] relative to the Greenland ice core record, thereby dating the onset of the Younger Dryas at 12,807 ± 12 cal BP, around 130 years earlier than thought. Our results synchronise the Younger Dryas across the North Atlantic-European sector, preclude a direct link between the LSE and Greenland Stadial-1 cooling[7], and suggest a large-scale common mechanism of a weakened Atlantic Meridional Overturning Circulation under warming conditions[8-10].

The Laacher See eruption (LSE) in central Germany expelled around 20 km^3 of tephra[1], making it comparable in magnitude to the 1991 eruption of Mount Pinatubo[11]. Proximal areas were buried by thick pumice fall deposits and ignimbrites[12] (Fig. 1), while Laacher See tephra (LST) fallout from ash clouds reached Northern Italy and Saint Petersburg (Extended Data Fig. 1), yielding a distinctive marker bed recognised in terrestrial and lacustrine records[3]. The generally accepted age of the eruption of 12,880 ± 40 BP$_{\mathrm{MFM}}$ (before 1950) derives from the Meerfelder Maar (MFM) varve record[5]. Further estimates are associated with much higher uncertainties and define a time window for the eruption of circa 13,200–12,840 years BP (ref. [4]). The only independent age estimate was obtained from radiometric (^{40}Ar/^{39}Ar) dating of the Upper LST deposits (12,900 ± 560 BP)[13] but it suffers from considerable uncertainty. Owing to its widespread dispersal, the LST represents a decisive Late Glacial isochron, enabling synchronization of proxy archives over a wide area[3]. While evidence for the eruption's regional environmental impacts is well documented[2], its influence on Northern Hemisphere climate is ambiguous, owing in part to poor constrains of its sulphur yield to the atmosphere (estimates range between 7 and 300 Tg of sulphur dioxide[2,14]).

What is clear is that the eruption took place during the later phase of the Allerød (AL) interstadial, and circa 200 varve-counted years before the onset of the Younger Dryas (YD) cold interval[12]. Despite decades of intensive research, the lingering dating uncertainty for the LSE has limited the development of an absolutely-dated European Late Glacial proxy chronology, intercomparison of European terrestrial and Arctic glaciochemical records, and evaluation of the North Atlantic climate transition from the Late Glacial to the early Holocene, including the speculated role of the LSE in triggering Greenland Stadial 1 (GS-1)[7]. However, the development of a high temporal resolution radiocarbon (^{14}C) calibration curve based on Late Glacial subfossil trees from Switzerland[15] paved the way for progress in dating the LSE, leading us to conduct new dendrochronological and ^{14}C dating studies of subfossil trees that were killed during the eruption and engulfed in its deposits. This approach provides the first independent and absolute calibration of various Late Glacial proxy archives.

Multi-parameter dating

We examined three birch (*Betula* sp.) and two poplar *(Populus* sp.) trunks found in LSE deposits near the crater (see Methods, Fig. 1 and Extended Data Fig. 2). *Poplar 1* is the only non-carbonized sample, and therefore suitable for macroscopic tree-ring width measurements (see Methods). Wood anatomical thin sectioning[16] and X-ray densitometry[17] of the charcoal samples allowed precise identification of ring boundaries (online Supplementary Table 1) and dendrochronological cross-dating. Determination of the LSE age was supported by the presence of the outermost ring and bark. *Birch 1* and *Poplar 1* contained 104 and 95 tree rings, respectively (Fig. 2 and Extended Data Table 1). The presence of initial early wood cells prior to the bark on *Poplar 1* corroborates previously reported sedimentological, palaeobotanical and trace fossil evidence for a spring/early summer eruption[12].

We performed 157 high-resolution ^{14}C measurements (see Methods) for *Birch 1*, *Poplar 1* and *Poplar 2* (Extended Data Table 1 and Supplementary Table 2-4). Wiggle-matching of the new ^{14}C values from our 104-year-long pre-LSE tree-ring chronology against the Swiss Late Glacial Master Radiocarbon dataset (SWILM-^{14}C; see Methods, Extended Data Fig. 3 and Supplementary Table 8)[15,18] dates the LSE to 13,006 ± 9 cal BP (2σ; Fig. 3a). Agreement of high and low frequency $\Delta^{14}C$ changes from 13,111–13,007 cal BP between the highly resolved isotopic measurements from the pre-LSE sequence and SWILM-^{14}C reference constrains the uncertainty. Note in Fig. 3a that the rapid increase in ^{14}C between 13,110 and 13,090 cal BP positions the pre-LSE sequence precisely and does not allow for ambiguity. The ^{14}C excursion centred at 13,055 cal BP not only validates the dating between the birch and poplar data, but also supports synchronisation relative to the SWILM-^{14}C record.

North Atlantic-European archives

Our new LSE age, circa 130 years older than hitherto reported, contributes to an independent, near-absolute tephrostratigraphic tie-point for the Late Glacial, and sheds new light on the controversial debate of the timing, pace, duration and spatiotemporal transgression of North Atlantic climate changes. The transition from the Late Glacial to early Holocene is characterized by strong climatic and environmental fluctuations, including the ~1100-year-long YD, the last severe cold reversal before the Holocene[19-23]. The onset of the YD is recognised as time-transgressive in European proxy archives, indicating regional and delayed responses to climatic changes that are recorded earlier in Greenland ice cores[24-26]. Acknowledging different sampling resolutions and dating uncertainties of the various archives, the offset between Greenland GS-1 and the European YD has been estimated to be up to two centuries[6,27].

The new LSE age of 13,006 ± 9 cal BP shifts many European proxy records to older ages and challenges the previously hypothesized delayed and stepwise southward migration of the YD (Extended Data Fig. 4a)[6]. The varved lake sediments from MFM, which is ~50 km southwest of Laacher See, represent the most reliable master chronology for the YD in central Europe[5]. This record places the LSE at 12,880 ± 40 $\mathrm{BP_{MFM}}$ (ref. [5]). However, the MFM chronology depends on the Ulmener Maar Tephra dated at 11,000 varve years BP and single ^{14}C dates[28], challenging its derived LST date. Our new LSE age shifts the MFM record by 126 years towards older ages during the late AL. Since ~200 varve years have been recorded consistently in annually-resolved European varved records between the LSE fallout horizon and the beginning of the YD[19,29-31], the onset of the YD is necessarily revised to 12,807 ± 12 years BP (2σ; see Methods and Extended Data Table 2).

The beginning of GS-1 cooling is dated at 12,846 (± 138 years) $\mathrm{BP_{GICC05}}$ (ref. [32]) years before 1950 on the Greenland Ice Core Chronology 2005 timescale (GICC05; Extended Data Fig. 4a)[23]. Our revised older age for the YD onset recorded in the European lakes now aligns with the Greenland Interstadial 1a / Greenland Stadial 1 (GI-1a/GS-1) transition (Fig. 4b-d), and thus synchronizes the onset of GS-1 and the YD. Based on the synchronization of tree-ring ^{14}C and ice core beryllium-10 (^{10}Be), both timescales are consistent within about -12/+21 years (2σ) around this period in time[33]. This synchronization thereby bypasses the cumulative counting error of the ice core timescale for the GS-1 versus YD comparison. Stable oxygen isotope ($\delta^{18}O$) measurements of sediment cores from the European Alpine lakes Ammersee[34] and Mondsee[35], both containing LST, are based on age models that incorporate the LSE age from MFM. Revising these models with our new LSE age shows that the isotopic AL/YD transition is synchronous with the climate transition in Greenland (Fig. 4c,d). Identification of LSE tephra in Greenland ice cores would yield the first near-absolute time marker of the pre-Holocene GICC05 chronology. Correcting for differences between tree-ring and ice-core timescales within this period[33], the new LSE age now confines the search window in ice cores to a range between 13,015 and 12,975 years BP_{GICC05} (see Methods; Extended Data Fig. 5 and Extended Data Table 3).

Atlantic-European climate mechanisms

Our study demonstrates for the first time that the Greenland GI-1/GS-1 transition coincided with the European AL/YD cooling. The temporal match between Greenland ice core and central European climate proxies implies that the last major Northern Hemisphere cooling interval before the Holocene was initiated and steered by an abrupt climate system change that instantly affected the whole North Atlantic region. This finding is in line with a revised calibration of ^{14}C data from Kråkenes Lake in western Norway (Fig. 4b)[26,36] using the 2020 International Radiocarbon Calibration Curve IntCal20 (ref. [18]). The improved calibration (Extended Data Table 4) shows that the AL/YD boundary in Scandinavia coincides with the proposed AL/YD transition in lacustrine varve records from Central Europe (see Methods). Our results further rule out any direct impact of the LSE on the transition into GS-1, as suggested previously[7], since the revised eruption substantially precedes the cooling identified in Greenland ice core records[32].

The trigger of the GS-1 cold reversal has been attributed to a sudden meltwater release from the Laurentide Ice Sheet in North America that weakened the Atlantic Meridional Overturning Circulation (AMOC)[8]. Understanding the exact timing of such a large-scale climate transition is important in the context of recent global warming, which is also characterized by a weakened AMOC[9]. The GS-1/YD cold reversal, therefore, represents a natural analogue to the predicted consequences of a weakened AMOC under global warming[9-10]. The improved proxy synchronisation arising from our ^{14}C-tuned dating of the LSE promises improved insights into the triggers and extent of the YD[8,37,38], which may, in turn, inform understanding of the conditions conducive to any future AMOC shutdown.

References

1. Schmincke, H.-U. The Quaternary volcanic fields of the east and west Eifel (Germany). in *Mantle plumes* 241–322 (Springer, 2007).
2. Schmincke, H.-U., Park, C. & Harms, E. Evolution and environmental impacts of the eruption of Laacher See Volcano (Germany) 12,900 a BP. *Quat. Int.* **61**, 61–72 (1999).
3. Lane, C. S., Blockley, S. P. E., Bronk Ramsey, C. & Lotter, A. F. Tephrochronology and absolute centennial scale synchronisation of European and Greenland records for the last glacial to interglacial transition: A case study of Soppensee and NGRIP. *Quat. Int.* **246**, 145–156 (2011).
4. Reinig, F. *et al.* Towards a dendrochronologically refined date of the Laacher See eruption around 13,000 years ago. *Quat. Sci. Rev.* **229**, 106128 (2020).
5. Brauer, A., Endres, C. & Negendank, J. F. W. Lateglacial calendar year chronology based on annually laminated sediments from Lake Meerfelder Maar, Germany. *Quat. Int.* **61**, 17–25 (1999).

6. Rach, O., Brauer, A., Wilkes, H. & Sachse, D. Delayed hydrological response to Greenland cooling at the onset of the Younger Dryas in western Europe. *Nat. Geosci.* **7**, 109–112 (2014).
7. Baldini, J. U. L., Brown, R. J. & Mawdsley, N. Evaluating the link between the sulfur-rich Laacher See volcanic eruption and the Younger Dryas climate anomaly. *Clim. Past* **14**, 969–990 (2018).
8. Broecker, W. S., Peteet, D. M. & Rind, D. Does the ocean–atmosphere system have more than one stable mode of operation? *Nature* **315**, 21–26 (1985).
9. Rahmstorf, S. *et al.* Exceptional twentieth-century slowdown in Atlantic Ocean overturning circulation. *Nat. Clim. Change* **5**, 475–480 (2015).
10. Caesar, L., Rahmstorf, S., Robinson, A., Feulner, G. & Saba, V. Observed fingerprint of a weakening Atlantic Ocean overturning circulation. *Nature* **556**, 191–196 (2018).
11. Holasek, R. E., Self, S. & Woods, A. W. Satellite observations and interpretation of the 1991 Mount Pinatubo eruption plumes. *J. Geophys. Res.* **101**, 27635–27655 (1996).
12. Baales, M. *et al.* Impact of the Late Glacial eruption of the Laacher See volcano, central Rhineland, Germany. *Quat. Res.* **58**, 273–288 (2002).
13. van den Bogaard, P. ^{40}Ar/^{39}Ar ages of sanidine phenocrysts from Laacher See Tephra (12,900 yr BP): Chronostratigraphic and petrological significance. *Earth Planet. Sci. Lett.* **133**, 163–174 (1995).
14. Textor, C., Sachs, P. M., Graf, H.-F. & Hansteen, T. H. The 12 900 years BP Laacher See eruption: estimation of volatile yields and simulation of their fate in the plume. *Geol. Soc. Lon. Spec. Pub.* **213**, 307–328 (2003).
15. Reinig, F. *et al.* New tree-ring evidence for the Late Glacial period from the northern pre-Alps in eastern Switzerland. *Quat. Sci. Rev.* **186**, 215–224 (2018).

16. Reinig, F. *et al.* Introducing anatomical techniques to subfossil wood. *Dendrochronologia* **52**, 146–151 (2018).

17. Schweingruber, F. H. *Tree Rings: Basics and Applications of Dendrochronology*. (1988).

18. Reimer, P. J. *et al.* The IntCal20 Northern Hemisphere radiocarbon age calibration curve (0-55 kcal BP). *Radiocarbon* 1–33 (2020).

19. Brauer, A., Haug, G. H., Dulski, P., Sigman, D. M. & Negendank, J. F. W. An abrupt wind shift in western Europe at the onset of the Younger Dryas cold period. *Nat. Geosci.* **1**, 520–523 (2008).

20. Haflidason, H., Petter Sejrup, H., Klitgaard Kristensen, D. & Johnsen, S. Coupled response of the late glacial climatic shifts of northwest Europe reflected in Greenland ice cores: Evidence from the northern North Sea. *Geology* **23**, 1059–1062 (1995).

21. Hughen, K. A., Southon, J. R., Lehman, S. J. & Overpeck, J. T. Synchronous radiocarbon and climate shifts during the last deglaciation. *Science* **290**, 1951–1954 (2000).

22. Johnsen, S. J. *et al.* Irregular glacial interstadials recorded in a new Greenland ice core. *Nature* **359**, 311–313 (1992).

23. Rasmussen, S. O. *et al.* A stratigraphic framework for abrupt climatic changes during the Last Glacial period based on three synchronized Greenland ice-core records: refining and extending the INTIMATE event stratigraphy. *Quat. Sci. Rev.* **106**, 14–28 (2014).

24. Lane, C. S., Brauer, A., Blockley, S. P. E. & Dulski, P. Volcanic ash reveals time-transgressive abrupt climate change during the Younger Dryas. *Geology* **41**, 1251–1254 (2013).

25. Muschitiello, F. *et al.* Fennoscandian freshwater control on Greenland hydroclimate shifts at the onset of the Younger Dryas. *Nat. Commun.* **6**, 8939 (2015).

26. Obreht, I. *et al.* An annually resolved record of Western European vegetation response to Younger Dryas cooling. *Quat. Sci. Rev.* **231**, 106198 (2020).

27. Lohne, Ø. S., Mangerud, J. & Birks, H. H. Precise ^{14}C ages of the Vedde and Saksunarvatn ashes and the Younger Dryas boundaries from western Norway and their comparison with the Greenland Ice Core (GICC05) chronology. *J. Quat. Sci.* **28**, 490–500 (2013).

28. Brauer, A. *et al.* High resolution sediment and vegetation responses to Younger Dryas climate change in varved lake sediments from Meerfelder Maar, Germany. *Quat. Sci. Rev.* **18**, 321–329 (1999).

29. Neugebauer, I. *et al.* A Younger Dryas varve chronology from the Rehwiese palaeolake record in NE-Germany. *Quat. Sci. Rev.* **36**, 91–102 (2012).

30. Lotter, A. F., Eicher, U., Siegenthaler, U. & Birks, H. J. B. Late glacial climatic oscillations as recorded in Swiss lake sediments. *J. Quat. Sci.* **7**, 187–204 (1992).

31. Merkt, J. & Müller, H. Varve chronology and palynology of the Lateglacial in Northwest Germany from lacustrine sediments of Hämelsee in Lower Saxony. *Quat. Int.* **61**, 41–59 (1999).

32. Steffensen, J. P. *et al.* High-Resolution Greenland Ice Core Data Show Abrupt Climate Change Happens in Few Years. *Science* **321**, 680–684 (2008).

33. Adolphi, F. *et al.* Connecting the Greenland ice-core and U/Th timescales via cosmogenic radionuclides: testing the synchroneity of Dansgaard–Oeschger events. *Clim. Past* **14**, 1755–1781 (2018).

34. Von Grafenstein, U., Erlenkeuser, H., Brauer, A., Jouzel, J. & Johnsen, S. J. A Mid-European Decadal Isotope-Climate Record from 15,500 to 5000 Years B.P. *Science* **284**, 1654–1657 (1999).

35. Lauterbach, S. *et al.* Environmental responses to Lateglacial climatic fluctuations recorded in the sediments of pre-Alpine Lake Mondsee (northeastern Alps). *J. Quat. Sci.* **26**, 253–267 (2011).

36. Lohne, Ø. S., Mangerud, J. & Birks, H. H. IntCal13 calibrated ages of the Vedde and Saksunarvatn ashes and the Younger Dryas boundaries from Kråkenes, western Norway. *J. Quat. Sci.* **29**, 506–507 (2014).

37. Condron, A. & Winsor, P. Meltwater routing and the Younger Dryas. *Proc. Natl. Acad. Sci. U.S.A.* **109**, 19928–19933 (2012).

38. Renssen, H. *et al.* Multiple causes of the Younger Dryas cold period. *Nat. Geosci.* **8**, 946–949 (2015).

39. Hajdas, I. *et al.* AMS radiocarbon dating and varve chronology of Lake Soppensee: 6000 to 12000 ^{14}C years BP. *Clim. Dyn.* **9**, 107–116 (1993).

40. Wulf, S. *et al.* Tracing the Laacher See Tephra in the varved sediment record of the Trzechowskie palaeolake in central Northern Poland. *Quat. Sci. Rev.* **76**, 129–139 (2013).

Fig. 1 | Laacher See Eruption (LSE) wood finds. Location of (**a**) the Laacher See and (**b**) discovered subfossil wood samples (white circles) within the Middle Laacher See tephra (MLST) ignimbrite deposits (red shading) near Andernach, Germany (modified from ref. [12]). Subfossil tree (**c**) buried in a tuff quarry near Meurin (circle 1) and (**d**) near Miesenheim excavated in 2019 (circle 2). (**e**) X-ray densitometry image of a charcoal sample of *Birch 1* (circle 3). Map produced using QGIS.

Fig. 2 | Dendrochronological cross-dating of pre-Laacher See Eruption (LSE) Tree-Ring Width (TRW) measurements. (**a**) Two poplar and (**b**) three birch samples, aligned along the bark layer of *Poplar 1* and *Birch 3*. All the trees had been killed and buried during the LSE, and were excavated from tephra deposits. Note logarithmic scales.

Fig. 3 | Dating of the Laacher See Eruption (LSE). (**a**) High-resolution radiocarbon (^{14}C) measurements from three tree-ring sequences recovered from LST deposits and wiggle-matched to the Swiss Late Glacial reference SWILM-^{14}C on the ^{14}C timescale, cal BP (1950)[15,18]. Blue shading denotes to the 2020 International Radiocarbon Calibration Curve IntCal20 (ref. [18]). Data are shown with 1σ errors. (**b**) Tree-ring boundaries and bark identified macroscopically on *Poplar 1*.

Fig. 4 | Multi-proxy alignment of circum-Atlantic records. (**a**) NGRIP oxygen isotopes ($\delta^{18}O$; relative to Vienna Standard Mean Ocean Water standard) in 20-year (black)[23] and annual (grey)[31] resolution on the GICC05 timescale[23]. Light blue shading denotes the GI-

1a/GS-1 transition in $\delta^{18}O$, while the vertical grey dashed line marks the transition in deuterium excess[32]. (**b**) Temporal shift of the mean Meerfelder Maar LST age estimate (12,880 varve years BP)[28] by 126 years towards older ages. Mean (± 1σ) AL/YD boundary ages obtained from Kråkenes Lake (Norway,)[27] calibrated against IntCal20 (ref. [18]), and mean and standard deviation (purple bar) of European varved terrestrial records (Soppensee, Switzerland[39]; Rehwiese, Germany[29]; Trzechowskie, Poland[40]) aligned relative to our newly established LSE age estimate (red vertical line), consistently indicating approximately 200–213 annual varves (avl) between the LST and the AL/YD boundary, implying a YD onset at around 12,807 cal BP. (**c-d**) Realigned LST-containing Late Glacial alpine $\delta^{18}O$ records from Mondsee[35] and Lake Ammersee[34] (relative to Vienna PeeDee Belemnite standard). Arrows indicate the temporal shift of 126 years toward older ages. (a) is plotted according to the GICC05 timescale with respect to 1950, while (b-d) are plotted on the ^{14}C timescale cal BP (1950).

Methods

Sample provenance and description

An area of more than 1000 km³ was buried below LST[11]. Within approximately 10 km radius around the Laacher See, where LST fallout deposits and ignimbrites reached significant thicknesses, and of the lower Neuwied Basin, where temporarily lakes had syn-eruptively formed[41], finds of diaspores, plant macrofossils[12] and leaf imprints[42] document a species-rich interstadial Late Glacial hemiboreal vegetation. Over the past 200 years botanical macro remains have been randomly gathered, often by private collectors[42]. Since the 1950s material was sampled during geoscientific fieldwork and samples were submitted for radiocarbon dating[43,44]. Over the last 40 years, some tree macro-fossils were collected by different science institutes, i.e., at the universities of Cologne, Hohenheim and Duisburg-Essen. The most systematic collection is stored in the MONREPOS Archaeological Research Centre and Museum for Human Behavioural Evolution near Neuwied (Germany), a competence centre of the Römisch-Germanisches Zentralmuseum (RGZM), where material unearthed during extensive geoarchaeological work in and around the Neuwied Basin has been archived since the 1980s (Extended Data Fig. 2)[12,45,46]. During a recent field campaign in January 2019 well-preserved trees buried within LST ignimbrites (ignimbrites and co-ignimbrites of the Middle LST deposits: MLST) were documented at a new locality near Miesenheim.

Within the more loosely packed pumice fallout deposits molds of trees still standing upright have been observed frequently[41], whereas in situ subfossil and/or charred trees were only preserved within the compact ignimbritic MLST deposits[47]. These filled the pre-LSE near-vent valleys and depressions by approximately 10-20 m thick deposits to the south and south-east of the Laacher See (Nette Valley ignimbrites) and up to 60 m to the north and north-east

(Brohl Valley ignimbrites) during the middle phase of the LSE (Fig. 1 and Extended Data Fig. 2). At some localities such as in Brohl, sites 1 and 2 (ref. [45]), and in Kruft[47] smaller stands of trees were documented during roadwork and quarrying, respectively, and excavated using archaeological methods. At the site Miesenheim 2 (ref. [12]), an entire forest floor with poplar tree stems and roots was excavated and documented over an area of several hundred square meters in the mid-1980s[46]. At this site, however, the preserved wood was strongly mouldered which made it impossible to preserve. Other tree macro-fossils found at various sites within the region, include trees tilted by syn-eruptive blasts (and/or numerous charred wood fragments), as were first discovered at Thür[48]. Further such discoveries have been documented at Tönisstein and other Brohl Valley exposures, in the Meurin quarries near Kruft, in Miesenheim 4 and at the 2019 Miesenheim locality, where we were able to excavate and document a series of well-preserved tilted trees with diameters up to 20 cm, buried within MLST ignimbrites.

For the present study five tree samples (2 poplar and 3 birch trees) with the most intact wood quality and structure were chosen for tree-ring width (TRW) analysis (Supplementary Table 1). The samples, where more detailed information is available, consistently derive from trees that have been preserved and discovered within MLST deposits burying the trees at their immediate growth sites. In Miesenheim 2, Kruft, and in the Brohl Valley, trees were documented standing upright, embedded within basal MLST ignimbrites. With the succeeding ignimbrite flow through the valley, the trunks were capped at approximately 4 m length. The observed upright position and the occasional presence of bark on the tree samples indicate that the trees were still alive prior to their burial. Two subfossil tree finds made by monks and provided by the University of Duisburg-Essen, were most likely excavated during renovation works in the immediate vicinity around the monastery and must have been directly located within the LSE ignimbrites and/or the denser-packed co-ignimbritic (s.c. “Trass”-) layers within the pumice fallout deposits (both types of deposits are assigned to the MLST), given their excellent preservation. The same must be assumed for a sample retrieved from an excursion and made available by the University of Hohenheim. Intrusion of material can be excluded, given the thickness of LST deposits, the late Allerød ^{14}C-dates and the preservation status of the samples studied. Conservation within the dense ignimbrites enabled the recovery of the bark on two samples (Extended Data Table 1), still attached to the outer sapwood. With the exception of *Poplar 1* with still intact wood cellulose, the preserved tree samples have been carbonized within the compact and hot ignimbrites.

TRW measurement and cross-dating

At the Swiss Federal Research Institute for Forest, Snow and Landscape WSL in Birmensdorf (Switzerland) wood anatomical transverse (cross) sections were taken, classifying the charcoal samples either as birch (*Betula* sp.) or poplar *(Populus* sp.). Exact tree-ring boundaries are often difficult to identify in broadleaved species and classical microscopic measurements were hindered through narrow rings and the carbonized sample status. Ensuring accurate tree-ring boundary identification, wood anatomical thin sectioning[16] as well as X-ray densitometry[17] were applied. Thin sections provided insight into the outer tree-ring identification, whereas X-ray images of carefully cut 0.2–0.5 cm thick discs enabled multi-radii measurements across the samples. At least four TRW radii were measured from each charcoal sample using a LINTAB measuring device with a precision of 0.01 mm in combination with TSAPWin software[49]. X-ray films were measured on a Walesch 2003 X-ray densitometer using WalDendro V1.10 software, equally with a precision of 0.01 mm. Visual cross-dating was performed within TSAPWin software[49]. Macroscopic TRW measurements of *Poplar 1* were performed at the University of Hohenheim with an identical measurement set-up as at WSL.

Radiocarbon sample preparation and measurement

Based on the cross-dated TRW sequences, 0.8–1.0 cm wide wood tracks were cut from three tree samples (*Poplar 1*, *Poplar 2* and *Birch 1*), including the pith and outer most rings of each tree. Rings were manually cut with a scalpel, if possible, in annual or bi-annual resolution providing at least 20 mg of organic material. Special care was taken to prevent any contamination, particularly from neighbouring tree rings. High-resolution radiocarbon (^{14}C) Accelerator Mass Spectrometer (AMS) measurements[50-52] were performed at the Laboratory of Ion Beam Physics at ETH Zurich (Switzerland) on the "Mini Radiocarbon Dating System" (MICADAS). The base-acid-base-acid-bleach method[53] was cautiously applied to extract holocellulose from the intact wood samples. The same treatment was applied to the delicate charcoal samples to isolate the most stable compounds from any external contamination for radiocarbon dating. All samples were, thereafter, graphitized with an AGE system[53]. The ETH quality protocol[54] was applied to ensure the accuracy and comparability of the ^{14}C results through continuous monitoring of ^{14}C blanks, standards and reference material.

Swiss radiocarbon reference dataset

The collection of subfossil Late Glacial wood from Switzerland[15] and corresponding atmospheric ^{14}C level changes data set, SWILM-^{14}C (ref. [18]), provides a well-dated (± 8 years; 2σ) and temporally high resolved reference for precise ^{14}C matching. Compared to the recently released International Calibration Curve 2020 (IntCal20)[18], the SWILM-^{14}C record, solely derived from a single long-lived tree from this period, GAEN0071 (Supplementary

Table 5), represents a record with higher temporal resolution. Additionally, 118 ^{14}C measurements from two trees (Supplementary Table 6 and 7) originating from the Swiss tree-ring chronology *Daettnau 3* (ref. [55]), enabled to match the pre-LSE tree-ring ^{14}C data to an extended reference, termed SWILM-^{14}C$_{plus}$. It is important to note that the dendrochronological placement of *Daettnau 3* to the *SWILM-^{14}C* record is tentative. Thus, we consider the matching results to the SWILM-^{14}C$_{plus}$ record only as an additional test to the results obtained from the SWILM-^{14}C data.

Radiocarbon wiggle-matching with OxCal

For the ^{14}C calibration, 85 ^{14}C measurements from *Poplar 1* were wiggle-matched against both, the SWILM-^{14}C and the extended SWILM-^{14}C$_{plus}$ records using the *D_Sequence* function in OxCal 4.3 (see dating results for *Poplar 2* and *Birch 1* below)[56,57]. The calibration curve was built applying a Savitzky-Golay filter (order: 2; frame length:11) and the possible offset was set to ± 50 years. The wiggle-matching analysis indicates overall good agreement of all *Poplar 1* ^{14}C dates to the SWILM-^{14}C reference, dating the outermost ring of the sample to 13,007 (± 1 year; 2σ). Calibration of *Poplar 1* with SWILM-^{14}C$_{plus}$ indicates 13,006 (± 1 year; 2σ) as the date of the final ring. Taking into account the underlying reference uncertainty of ± 8 years of the SWILM-^{14}C record, we obtain an absolute uncertainty of ± 9 years for both wiggle-matches. OxCal results for *Birch 1* and *Poplar 2* support this wiggle-match (Extended Data Fig. 6).

Radiocarbon wiggle-matching with a least square fit

In addition to wiggle-matching results from OxCal, ^{14}C sampled trees from the pre-LSE tree-ring chronology were matched to the SWILM-^{14}C and SWILM-^{14}C$_{plus}$, such that the chi-square $(\chi(x)^2)$ becomes minimal for an assumed age x for the outermost tree ring (waney edge) prior to the eruption[52]:

$$\chi(x)^2 = \sum_{i=1}^{n} \frac{\left(R_i - \bar{C}_{(x-r_i)} - offset\right)^2}{\left(\delta R_i^2 + \delta \bar{C}_{(x-r_i)})^2\right)}$$

where $R_i \pm \delta R_i$ are the measured values for the measured ^{14}C concentrations of the sample and $\bar{C}_{(x-r_i)} \pm \delta \bar{C}_{(x-r_i)}$ represents the ^{14}C concentrations of the SWILM-^{14}C curve for the year $(x - r_i)$, where r_i is the tree-ring number starting with ring number 0 as the final ring of the tree. The $(\chi(x)^2)$ for the most likely matches are given in Extended Data Fig. 3. When tree rings were sampled in lower temporal resolution, ^{14}C values of the trees with higher resolution were combined to match the lower resolution for the chi-square test. The offset was individually adjusted to find the overall best fit.

Radiocarbon dating uncertainty

The application of the Oxcal *D_Sequence* function and the least chi-square test yield similar results, indicating an LSE age of 13,006 (± 9 years; 2σ). We consider our result as robust, as testing various combinations between samples and references produce age estimates within the derived age error. While ^{14}C measurements from *Poplar 1,* originating from whole wood, indicate most significant dating results, ^{14}C measurements from the carbonized wood of *Birch 1* indicates a systematic offset. Nevertheless, the measurements follow the overall ^{14}C structure and outline similar LSE age estimates. We speculate that the observed systematic offset of the charcoal sample is either a result of the direct carbonization process within the hot LSE sediments, later contamination during preservation[58], or related to the injection of magmatic carbon dioxide into the samples during its lifetime, for example through regional groundwater affected by volcanic processes[59]. Dating results from carbonized *Poplar 2* are consistent with *Poplar 1*. We deduce the only offset between the samples in the period between 13,090 cal BP and 13,075 cal BP to the poor wood quality of the *Poplar 1* tree rings, where only selected years could be sampled and ^{14}C measurements performed. Precise ^{14}C placements were only feasible through the unique high-resolution of performed ^{14}C measurements and subsequent insight into the ^{14}C fine structure. Additionally, the now obtained number of tree rings more than 100 years prior to the eruption is crucial to exceed the ^{14}C plateau, a critical aspect which previous ^{14}C dating attempts of charcoal remnants found within the LSE deposits, did not achieve[60].

YD onset estimation

The revised date of the LSE now enables to more precisely estimate the onset of the YD to approximately 12,807 BP (± 12 years; 2σ), based on the standard deviation of the available counting uncertainties of annually laminated lake sediment records containing LSE evidence as well as high-resolution palaeobotanical evidence indicating the YD onset (Extended Data Table 2). We recognize that our result is, however, limited, by the systematic error based on the individual record and sampling strategy defining the YD onset. The shift in sedimentation in the Meerfelder Maar record indicates a sharp transition into the YD[5]. Defining the YD onset in pollen records is subject to (i) where the pollen samples are placed, (ii) what the pollen sampling resolution is, and (iii) how fast vegetation actually responded to climate deterioration. A lag of the pollen signal relative to the climatic shift can be expected, as the ecosystem response presumably occurred delayed[61]. For example, pollen-percentage diagrams from the Meerfelder Maar outline a slower transition compared to pollen accumulation rates, reflecting a more immediate response to the onset of the YD[62]. The chronological accuracy of

AL/YD palaeo-records is now reaching a point where it is actually more precise than the sampling resolution of the underlying proxy information, challenging previous sampling strategies. Moreover, the restricted number of published counting uncertainties within various archives hampers a more accurate age estimate. As long as no additional information on counting uncertainties within the individual records is available, applying the standard deviation of circa 2.7 % (5.6 years; Extended Data Table 2) covers the known systematic uncertainties and represents the most reliable error estimate of the YD onset in western and central Europe.

Ice-core assessment of LSE candidates

Volcanic eruption chronologies are commonly derived from increased ice acidity, tephra layers and/or anomalously high sulphate (or sulphur) concentrations measured in polar ice cores[63]. Several ice-core records from Greenland and Antarctica have previously been aligned by identifying common volcanic sulphate peaks[64] (Extended Data Fig. 5). Comparisons between tree-ring ^{14}C and ice core ^{10}Be data allows identification of leads and lags between these two timescales considering similar cosmogenic production rates[33,65-67]. Based on new high-resolution tree-ring data the ^{14}C timescale has recently been anchored at a precision of ± 8 years (2σ) during the AL/YD transition[18], whereas the accumulated age error is ±140 years for GICC05 in 13,000 BP_{GICC05} (ref. [23]). However, the absolute dating can be further constrained using cosmogenic isotopes. Best fit is commonly produced if GICC05 is shifted towards younger ages by 1-year (-12; +25 years; 2σ)[33]. Considering these refined uncertainties, the new LSE age now limits the search window for LSE fallout to 13,015–12,975 years BP_{GICC05} (Extended Data Fig. 5). This excludes the bipolar sulphur anomaly at

12,870 BP_{GICC05} (ref. [64]), tentatively linked to the LSE[7] and two other major bipolar eruption signals (Extended Data Table 3).

Zooming into the 13,015–12,975 BP_{GICC05} period, a high-resolution (1 cm) sulphate record[68] from the North Greenland Ice Core Project (NGRIP)[69] ice core depicts several candidate eruptions in this time window (Extended Data Fig. 5 and Extended Data Table 3). The youngest of these, referring to a bipolar sulphate deposition[64] in 12,980 $BP_{GICC05,}$ would imply an excessive gas content of the pre-eruption magma reservoir unlikely for the LSE. Two years earlier, in 12,982 BP_{GICC05}, a particle-rich signal also appears unlikely as the composition of glass shards does not match LSE phonolite[70]. Other depositions of insoluble particles[70] and volcanic acids[68] during this time window, recognized for some of the other candidate events (Extended Data Fig. 5 and Extended Data Table 3), present testable hypotheses for future ice-core research. A targeted search for cryptotephra offers the strongest chance of identifying the LSE signature in glacial archives.

Calibration of Kråkenes Lake ^{14}C data

Kråkenes Lake in western Norway[27,36] represents an important independent lacustrine archive of past environmental change and is independently dated using a total of 118 accelerator mass spectrometry ^{14}C dates performed covering the period from the AL to the early Holocene. This unique dataset enables independent determination of ^{14}C ages for the significant events around the YD cold spell, i.e., the AL/YD and the YD-Holocene transitions, as well as interstratified YD Vedde and early Holocene Saksunarvatn ash layers. Radiocarbon calibration of Kråkenes Lake ^{14}C ages using the *D_Sequence* function in OxCal[56,57] and applying the recently released IntCal20 (ref. [18]) dates the AL/YD transition to 12,840–12,699 cal BP (12,770 ±71; 2σ), indicating a shift of the median age estimate by approximately 54 years to older ages compared to IntCal13 (ref. [71]) (Extended Data Table 4). The revised AL/YD transition age estimate for Kråkenes Lake coincides with the proposed date based on the revised LSE age estimate and the consistent 200–213 varve years-long interval from the LSE tephra to the onset of the YD in annually layered records from western and central Europe. The calibrated dates of Vedde (12,153–11,935 cal BP; 12,044 ±109; 2σ) and Saksunarvatn (10,254–10,074 cal BP; 10,164 ±90; 2σ) ashes to IntCal20 (ref. [18]) remain consistent within errors to the results obtained using the IntCal13 (ref. [71]) calibration curve (Extended Data Table 4), as only minor adjustments of the calibration curve were made over this time interval.

Extended References

41. Park, C. & Schmincke, H.-U. Multistage damming of the Rhine River by tephra fallout during the 12,900 BP Plinian Laacher See Eruption (Germany). Syn-eruptive Rhine damming I. *J. Volcanol. Geotherm. Res.* **389**, 106688 (2020).
42. Waldmann, G. *Vulkanfossilien im Laacher Bims*. (Gregor and Unger, 1996).
43. Frechen, J. Die Tuffe des Laacher Vulkangebietes als quartärgeologische Leitgesteine und Zeitmarken. *Fortschritte der Geologie in Rheinland und Westfalen* **4**, 363–370 (1959).
44. Schweitzer, H.-J. Entstehung und Flora des Trasses im nördlichen Laachersee-Gebiet. *E&G Quaternary Science Journal* **9.1**, 28–56 (1958).
45. Street, M. Analysis of Late Palaeolithic and Mesolithic faunal assemblages in the northern Rhineland, Germany. (The University of Birmingham, Birmingham, 1993).
46. Street, M. Ein Wald der Allerodzeit bei Miesenheim, Stadt Andernach (Neuwieder Becken). *Archäologisches Korrespondenzblatt* **16.1,** 13–22 (1986).
47. Baales, M., Bittmann, F. & Kromer, B. Verkohlte Bäume im Trass der Laacher See-Tephra bei Kruft (Neuwieder Becken): Ein Beitrag zur Datierung des Laacher See-

Ereignisses und zur Vegetation der Allerød-Zeit am Mittelrhein. *Archäologisches Korrespondenzblatt* **28**, 191–204 (1998).

48. Brunnacker, K. *et al.* Spätpaläolithische Funde aus Thür, Kreis Mayen Koblenz. *Archäologisches Korrespondenzblatt Mainz* **12.4**, 417–427 (1982).
49. Rinn, F. *TSAP - time series analyses presentation. Referenz manual* (version 3.0). RinnTech, Heidelberg. (1996).
50. Synal, H.-A., Stocker, M. & Suter, M. MICADAS: A new compact radiocarbon AMS system. *Nucl. Instrum. Methods Phys. Res. B* **259**, 7–13 (2007).
51. Wacker, L. *et al.* MICADAS: Routine and High-Precision Radiocarbon Dating. *Radiocarbon* **52**, 252–262 (2010).
52. Wacker, L. *et al.* Radiocarbon Dating to a Single Year by Means of Rapid Atmospheric ^{14}C Changes. *Radiocarbon* **56**, 573–579 (2014).
53. Němec, M., Wacker, L. & Gäggeler, H. Optimization of the Graphitization Process at Age-1. *Radiocarbon* **52**, 1380–1393 (2010).
54. Sookdeo, A. et al. Quality dating: A well-defined protocol for quality high-precision ^{14}C-dates tested on Late Glacial wood. Radiocarbon **62**, 1–9 (2019).
55. Kaiser, K. F. *Beiträge zur Klimageschichte vom späten Hochglazial bis ins frühe Holozän: rekonstruiert mit Jahrringen und Molluskenschalen aus verschiedenen Vereisungsgebieten*. (Ziegler, 1993).
56. Bronk Ramsey, C. Deposition models for chronological records. *Quat. Sci. Rev.* **27**, 42–60 (2008).
57. Bronk Ramsey, C. Dealing with Outliers and Offsets in Radiocarbon Dating. *Radiocarbon* **51**, 1023–1045 (2009).
58. Bird, M. I. Radiocarbon Dating | Charcoal. in *Encyclopedia of Quaternary Science* 353–360 (Elsevier, 2013).

59. Holdaway, R. N., Duffy, B. & Kennedy, B. Evidence for magmatic carbon bias in ^{14}C dating of the Taupo and other major eruptions. *Nat. Commun.* **9**, 4110 (2018).

60. Kromer, B., Spurk, M., Remmele, S., Barbetti, M. & Joniello, V. Segments of Atmospheric ^{14}C Change as Derived from Late Glacial and Early Holocene Floating Tree-Ring Series. *Radiocarbon* **40**, 351–358 (1998).

61. Muschitiello, F. & Wohlfarth, B. Time-transgressive environmental shifts across Northern Europe at the onset of the Younger Dryas. *Quat. Sci. Rev.* **109**, 49–56 (2015).

62. Engels, S. *et al.* Subdecadal-scale vegetation responses to a previously unknown late-Allerød climate fluctuation and Younger Dryas cooling at Lake Meerfelder Maar (Germany). *J. Quat. Sci.* **31**, 741–752 (2016).

63. Sigl, M. *et al.* Timing and climate forcing of volcanic eruptions for the past 2,500 years. *Nature* **523**, 543–549 (2015).

64. Svensson, A. *et al.* Bipolar volcanic synchronization of abrupt climate change in Greenland and Antarctic ice cores during the last glacial period. *Clim. Past Discuss.* **2020**, 1-28 (2020).

65. Adolphi, F. & Muscheler, R. Synchronizing the Greenland ice core and radiocarbon timescales over the Holocene – Bayesian wiggle-matching of cosmogenic radionuclide records. *Clim. Past* **12**, 15–30 (2016).

66. Adolphi, F. *et al.* Radiocarbon calibration uncertainties during the last deglaciation: Insights from new floating tree-ring chronologies. *Quat. Sci. Rev.* **170**, 98–108 (2017).

67. Muscheler, R., Adolphi, F. & Knudsen, M. F. Assessing the differences between the IntCal and Greenland ice-core time scales for the last 14,000 years via the common cosmogenic radionuclide variations. *Quat. Sci. Rev.* **106**, 81–87 (2014).

68. Ruth, U., Wagenbach, D., Steffensen, J. P. & Bigler, M. Continuous record of microparticle concentration and size distribution in the central Greenland NGRIP ice core during the last glacial period. *J. Geophys. Res.* **108**, 1–12. (2003).

69. Bigler, M. *et al.* Optimization of High-Resolution Continuous Flow Analysis for Transient Climate Signals in Ice Cores. *Environ. Sci. Technol.* **45**, 4483–4489 (2011).

70. Mortensen, A. K., Bigler, M., Grönvold, K., Steffensen, J. P. & Johnsen, S. J. Volcanic ash layers from the Last Glacial Termination in the NGRIP ice core. *J. Quat. Sci.* **20**, 209–219 (2005).

71. Reimer, P. J. *et al.* IntCal13 and Marine13 Radiocarbon Age Calibration Curves 0–50,000 Years cal BP. *Radiocarbon* **55**, 1869–1887 (2013).

72. Buizert, C. *et al.* Abrupt ice-age shifts in southern westerly winds and Antarctic climate forced from the north. *Nature* **563**, 681–685 (2018).

73. Seierstad, I. K. *et al.* Consistently dated records from the Greenland GRIP, GISP2 and NGRIP ice cores for the past 104 ka reveal regional millennial-scale δ18O gradients with possible Heinrich event imprint. *Quat. Sci. Rev.* **106**, 29–46 (2014).

74. Sigl, M. *et al.* The WAIS Divide deep ice core WD2014 chronology – Part 2: Annual-layer counting (0–31 ka BP). *Clim. Past* **12**, 769–786 (2016).

75. Litt, T., Behre, K.-E., Meyer, K.-D., Stephan, H.-J. & Wansa, S. Stratigraphische Begriffe für das Quartär des norddeutschen Vereisungsgebietes. *Eiszeitalt. Ggw.* **56**, 7–65 (2007).

76. Riede, F. Past-Forwarding Ancient Calamities. Pathways for Making Archaeology Relevant in Disaster Risk Reduction Research. *Humanities* **6**, 79 (2017).

77. Patton, H. *et al.* Deglaciation of the Eurasian ice sheet complex. *Quat. Sci. Rev.* **169**, 148–172 (2017).

78. Zielinski, G. A., Mayewski, P. A., Meeker, L. D., Whitlow, S. & Twickler, M. S. A 110,000-Yr Record of Explosive Volcanism from the GISP2 (Greenland) Ice Core. *Quat. Res.* **45**, 109–118 (1996).

79. Severi, M. *et al.* Synchronisation of the EDML and EDC ice cores for the last 52 kyr by volcanic signature matching. *Clim. Past Discuss.* **3**, 409–433 (2007).

Acknowledgements This study was supported by the WSL-internal project "LSD" and the Swiss National Science Foundation (SNF Grant 200021L_157187/1). We would like to thank Angelika Hunold, Holger Schaaf and Benjamin Streubel from the Römisch-Germanisches Zentralmuseum (RGZM) competence centre for "Vulkanologie, Archäologie und Technikgeschichte" (VAT) in Mayen (Germany) for assistance during fieldwork, as well as the University of Hohenheim and Michael Friedrich for initial investigations during a DEKLIM-project. Finally, we would like to thank D. Dahl-Jensen and the three anonymous reviewers for their constructive feedback that further improved the quality of the manuscript.

Author contributions F.R., U.B., O.J. and L.W. designed the study with input from D.N. Tree-ring width measurements were performed by F.R., G.G., and D.N. Radiocarbon measurements and analyses were performed by G.G. and L.W., with the involvement of F.R., L.W. modelled the ^{14}C. The paper was written by F.R., together with U.B., O.J., J.E., C.O. and L.W. Further editorial contributions were obtained from F.A., P.C., S.E., C.L., M.S., A.S., H.-A.S., J.H.S. and R.W. Wood samples were prepared and provided by O.J., H.P., A.L. and S.R. Ice core data were provided and discussed by M.S. and F.A.

Corresponding author Correspondence to Frederick Reinig.

Competing interests The authors declare no competing interests.

Supplementary Information is available for this paper.

Data availability The supplementary information that support the findings of this study are available from XX, DOI:YY (DOI to be provided once embargo data is set). Source Data are provided with this paper.

Extended Data Table 1 | Pre-Laacher See Eruption (LSE) chronology. Dendrochronological characteristics and performed radiocarbon (^{14}C) measurements.

Extended Data Table 2 | Annually varved layers (avl) estimate of the YD onset relative to the LSE tephra (LST), including published information on counting uncertainty for all available annually laminated records in western and central Europe. Mean derived from the average of all records and their standard deviation.

Extended Data Table 3 | Volcanic sulphate depositions in Greenland[68] and Antarctica[74] around the new LSE date. Ice-core ages refer to the GICC05 chronology[23] with respect to 1950 derived from previous volcanic synchronizations[65,72,73].

Extended Data Table 4 | OxCal calibration results of ^{14}C-dated events from the Kråkenes core chronologies[27,36] using IntCal13 (ref. [71]) and IntCal20 (ref. [18]). Confidence Interval (CI), Mean, and Median are given in cal BP (1950).

Extended Data Fig. 1 | Temporal and spatial setting of the Laacher See eruption. (**a**) Climatic development of the last 15,000 years according to the NGRIP Greenland δ^{18}O ice core record (blue)[23], covering the Late Glacial and Holocene periods, shown together with the LST ^{40}Ar/^{39}Ar age determination at 12,900 ±560 BP (mean ±1σ; red)[13]. INTIMATE event stratigraphy[23] of the Late Glacial is outlined left of the NGRIP record (GS – Greenland Stadial; GI – Greenland Interstadial), with the European palaeobotanical subdivision of this period (MEI – Meiendorf interstadial; BØ – Bølling interstadial; AL – Allerød interstadial; YD – Younger Dryas cold interval)[75] aligned on its right. Offsets between both schemes are topic of intensive and ongoing discussion. (**b**) Geospatial distribution of LST fallout deposits (modified from ref. [76]) with locations of Laacher See (red triangle) and source of the tree stems used to build the Swiss Late Glacial tree-ring and ^{14}C records (green dot; SWILM-^{14}C)[18]. Light blue line indicates extent of late Allerød Fenno-Scandinavian ice sheet (modified from ref. [77]). Map produced using QGIS.

Extended Data Fig. 2 | Examples of Laacher See Eruption (LSE) wood finds. (**a**) Location of archived (circles with black borders) and newly excavated (in 2019, circles with orange borders) subfossil wood samples within the Middle Laacher See tephra (MLST) deposits in the Neuwied Basin (modified from ref. [12]). Isopachs for LST fallout are shown in red, and grey shading indicates extent of MLST ignimbrite deposits. Subfossil trees (**b**) from the Brohltal (1986 photo by E. Turner); (**c**) from an excavated forest at Miesenheim (1986 photo by M. Street)[46]; (**d**) from Kruft (1996 photo by M. Baales)[47]; (**e**) from Meurin; and (**f**) an excavation at a new locality in Miesenheim. Note that only samples from Brohltahl and Meurin are included in this study, as other materials were exhausted during previous analyses or unsuitable for the performed measurements (see Methods). Map produced using QGIS. All photos are provided by the MONREPOS picture archive.

Extended Data Fig. 3 | Reduced chi-square test results[52]. Most likely ^{14}C calendar placement of the last ring of *Poplar 1* matched to SWILM-^{14}C with an offset of 11 cal years (yrs) (**a**); *Poplar 1* matched to SWILM-^{14}C$_{\text{plus}}$ with an offset of 22 cal yrs (**b**); *Poplar 2* matched to SWILM-^{14}C with an offset of 18 cal yrs (**c**); *Birch 1* matched to SWILM-^{14}C with an offset of 36 cal yrs (**d**); *Birch 1* matched to SWILM-$^{14}C_{plus}$ with an offset of 46 cal yrs (**e**); all pre-LSE samples matched to SWILM-^{14}C with an offset of 20 cal yrs years (**f**); Daettnau 3 matched to SWILM-^{14}C with an offset of 13 cal yrs (**g**); and *Poplar 1* matched to Daettnau 3 with an offset of 25 cal yrs (**h**). Black lines denote to the 95% confidence interval.

Extended Data Fig. 4 | Multi-proxy alignment of North Atlantic and European records. (**a**) NGRIP (grey) and GISP2 (black) oxygen isotopes ($\delta^{18}O$) at 20-year resolution from Greenland on GICC05 timescale[23], Alpine $\delta^{18}O$ records from Lake Ammersee (yellow)[34] and Lake Mondsee (red)[35], and Meerfelder Maar (MFM, blue)[5] varve thickness plotted as 10-year running means, dated to the MFM timescale with a Laacher See eruption (LSE) date of 12,880 BP_{MFM} (± 40 years; red dotted vertical line) indicating time-transgressive Greenland Stadial 1 (GS-1) and the Younger Dryas (YD) cooling between 13,200 and 12,400 BP_{GICC05}. (**b**) The same European proxy records shifted 126 years according to the new LSE date of 13,006 cal BP (red vertical line)[28] now outlining a synchronized cooling into the GS-1/YD across the North Atlantic. Blue shading denotes the period of strongest cooling evident in the Greenland ice core isotope records.

Extended Data Fig. 5 | Non-sea salt sulphate and particle records from polar ice cores around the time of the LSE. (a) Ice-core records of sulphate from the Greenland Ice Sheet Project Two (GISP2)[78] and North Greenland Ice Core Project (NGRIP)[69] records; (**b**) High-resolution (1 cm depth) record of sulphate and dust[68] from the NGRIP ice-core record[69] between 13,015 and 12,975 years BP_{GICC05} with three volcanic anomalies at 12,980 BP_{GICC05} (1), 12,982 BP_{GICC05} (2), and 12,994 BP_{GICC05} (3); black arrows indicate additional obtained sulphate peaks; cyan bar denotes the 17 cm sampling range in which tephra shards were previously detected and characterized[70] encompassing two distinct volcanic signals (1 and 2); (**c**) ice-core records of sulphate (calculated from sulphur measurements) from West Antarctic Ice Sheet Divide (WD)[74] and Dronning Maud Land (EDML)[79] ice core. All ice-cores are synchronized[65,72,73] on the GICC05 chronology[23] timescale with respect to 1950. Grey vertical lines represent the accumulated age error in 13,000 BP with ±105 years for WD2014[74] and ±140 years for GICC05 (ref. [23]), which has been further reduced (-12/+25 years; 2σ) based on the synchronization of tree-ring ^{14}C and ice core ^{10}Be[33]. Red vertical lines outline the added LSE ^{14}C uncertainty (±9 years). Yellow dots denote to obtained bipolar sulphate anomalies.

Extended Data Fig. 6 | D_Sequence wiggle-matching results with OxCal. All radiocarbon (^{14}C) modelled LSE ages obtained from **(a)** *Poplar 1*, **(b)** *Birch 1* and **(c)** *Poplar 2* applying the extended Swiss Late Glacial Reference (SWILM-^{14}C$_{\text{plus}}$) point to a similar eruption date. While the long-lived *Poplar 1* and *Birch 1* exceed the ^{14}C plateau with the initial ^{14}C dates, *Poplar 2* provide three possible wiggle-match placements, however, under the contraint that this sample was also found within the MLST deposits the two younger ^{14}C results need to be excluded.

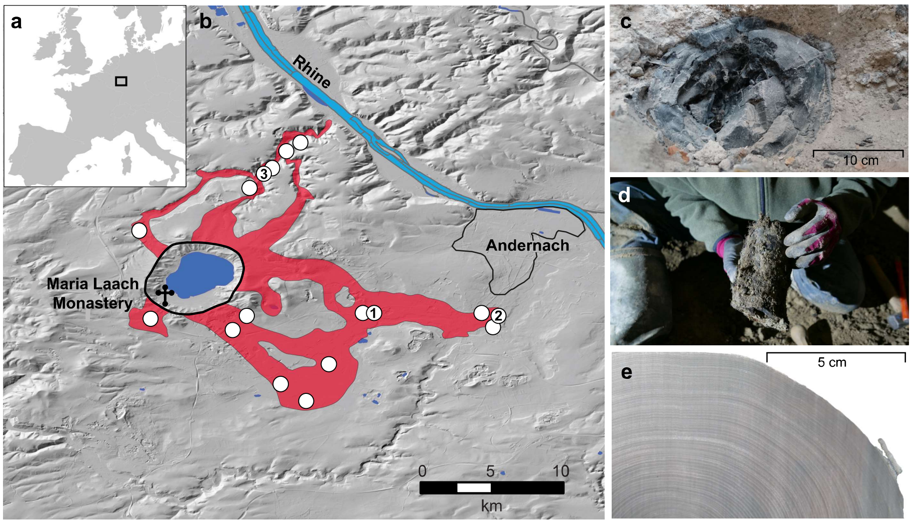
a
b
Rhine
Andernach
Maria Laach
Monastery
3
1
2
0
5
10
km
c
10 cm
d
e
5 cm

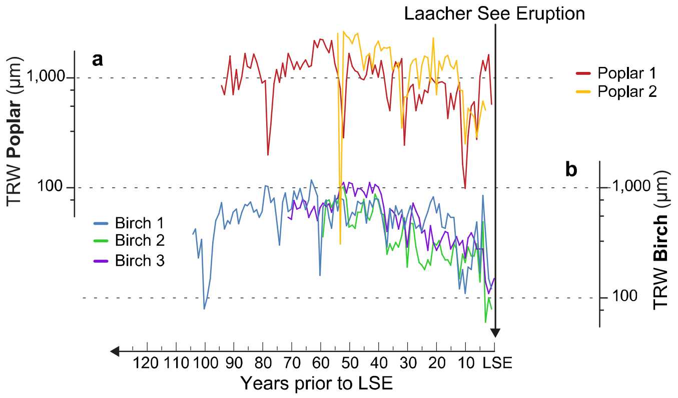
Laacher See Eruption
a
TRW **Poplar** (µm)
1,000
100
Poplar 1
Poplar 2
b
1,000
100
TRW **Birch** (µm)
Birch 1
Birch 2
Birch 3
120 110 100 90 80 70 60 50 40 30 20 10 LSE
Years prior to LSE

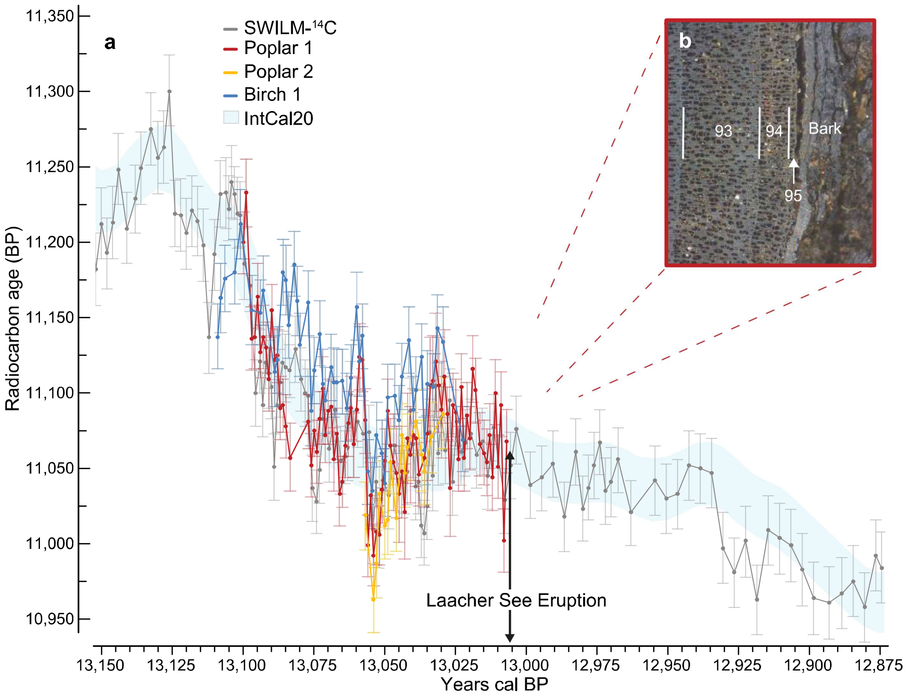
a
b
SWILM-14C
Poplar 1
Poplar 2
Birch 1
IntCal20
Radiocarbon age (BP)
11,350
11,300
11,250
11,200
11,150
11,100
11,050
11,000
10,950
Years cal BP
13,150
13,125
13,100
13,075
13,050
13,025
13,000
12,975
12,950
12,925
12,900
12,875
Laacher See Eruption
93
94
Bark
95

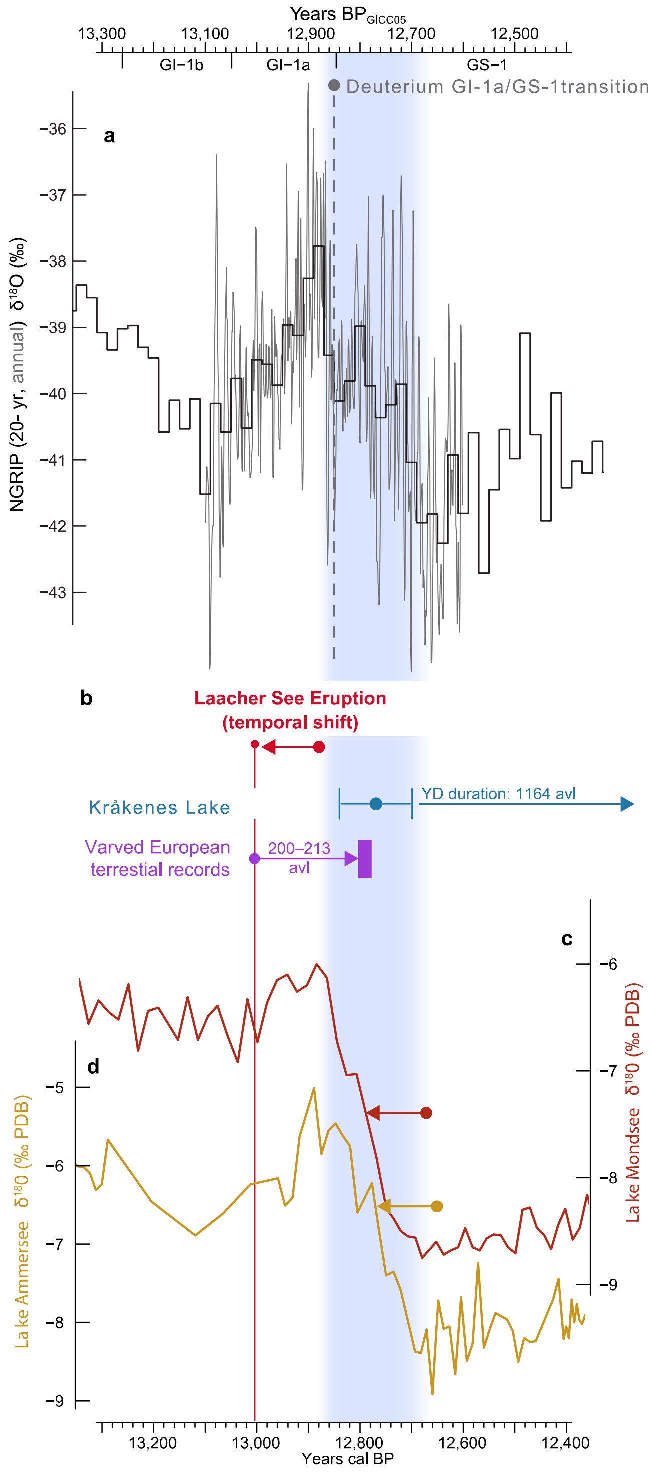
Years BP$_{GICC05}$
13,300
13,100
12,900
12,700
12,500
GI−1b
GI−1a
GS−1
Deuterium GI-1a/GS-1transition
a
NGRIP (20- yr, annual) δ^{18}O (‰)
−36
−37
−38
−39
−40
−41
−42
−43
b
Laacher See Eruption
(temporal shift)
Kråkenes Lake
YD duration: 1164 avl
Varved European
terrestial records
200–213
avl
c
−6
−7
−8
−9
Lake Mondsee δ^{18}0 (‰ PDB)
d
−5
−6
−7
−8
−9
Lake Ammersee δ^{18}0 (‰ PDB)
13,200
13,000
12,800
12,600
12,400
Years cal BP